Carbohydrate Polymers 81 (2010) 234–242

Contents lists available at ScienceDirect

Carbohydrate Polymers

journal homepage: www.elsevier.com/locate/carbpol

Chitosan microparticles incorporating a hydrophilic sunscreen agent

Yasmine A. Gomaa*, Labiba K. El-Khordagui[1], Nabila A. Boraei[2], Inas A. Darwish[3]

Department of Pharmaceutics, Faculty of Pharmacy, University of Alexandria, El-Khartoum square, Azarita, Alexandria 21521, Egypt

ARTICLE INFO

Article history:
Received 10 December 2009
Received in revised form 3 February 2010
Accepted 9 February 2010
Available online 4 March 2010

The paper was presented in the oral symposium of the Industrial Pharmacy Section, International Pharmaceutical Federation (FIP) Congress, Brazil, 2006

Keywords:
Organic sunscreen
Phenylbenzimidazole sulphonic acid
Chitosan
UV screening effect
Transpore™ tape
Crosslinking

ABSTRACT

A microparticulate delivery system incorporating the hydrophilic sunscreen agent, phenylbenzimidazole sulphonic acid (PBSA) was prepared for better in-use performance. Chitosan, not adequately considered for sunscreen delivery, was used a matrix material. Emulsion crosslinking with glutaraldehyde generated microparticles (MPs) with good features in terms of yield (≈76%), size (24–100 μm) and % incorporation efficiency (29–74%). PBSA release was sustained over 8 h according to a biphasic in-use relevant release pattern. The characteristics of PBSA-loaded chitosan MPs were determined by the interplay of the density of crosslinking of the chitosan matrix, particle size and chitosan–glutaraldehyde–PBSA interactions as evidenced by infrared and differential scanning calorimetric data. Incorporation of the sunscreen in chitosan MPs improved its in vitro UV screening effect using a model chitosan gel and Transpore™ tape. Accordingly, chitosan may be added to the platform of polymers suitable for the delivery of sunscreen actives, particularly hydrophilic agents.

1. Introduction

The use of sun protection products is growing tremendously as a result of recognition and increased public awareness of the adverse effects of UV solar radiation (Lautenschlager, Wulf, & Pittelkow, 2007). In-use criteria requirements of such products include mainly efficient protection against acute and long-term UV-induced skin damage, high skin accumulation of UV absorbers with minimal absorption, photostability of sunscreen actives, low skin irritation potential, user friendly application requirements such as desirable aesthetic attributes and reduced frequency of application (Forestier, 2008; Tanner, 2006). Conventional sunscreen formulations may fall short of meeting such criteria (González, Fernández-Lorente, & Gilaberte-Calzada, 2008). Recent research developments generally target the introduction of new broader spectrum organic UV absorbers (Fourtanier, Moyal, & Seité, 2008; Tuchinda, Lim, Osterwalder, & Rougier, 2006; Velasco et al., 2008), enhancing sunscreen photostability (Scalia & Mezzena, 2009; Tuchinda et al., 2006), improving the properties of inorganic filters by encapsulation and micronization (Nohynek, Lademann, Ribaud, & Roberts, 2007; Villalobos-Hernndez & Muller-Goymann, 2007), reducing skin penetration (Touitou & Godin, 2008), and designing new vehicles based on emerging controlled delivery technologies (Gogna, Jain, Yadav, & Agrawal, 2007; Iannuccelli, Sala, Tursilli, Coppi, & Scalia, 2006; Patel, Jain, Yadav, Gogna, & Agrawal, 2006). Such vehicles are multifunctional delivery systems that meet the criteria of effective sunscreen carriers.

As most organic UV filters are lipophilic compounds, solid lipid micro- and nanoparticles (Chunjin & Shuangxi, 2005; Tursilli, Piel, Delattre, & Scalia, 2007; Wissing & Müller, 2002; Xia, Saupe, Müller, & Souto, 2008) have been widely investigated as delivery systems. However, approved UV filters include hydrophilic agents which may need alternative matrix materials to enhance drug incorporation. Systems based on natural or synthetic polymers proved promising in this respect. For instance, incorporation of organic UV filters in gelatin (Patel et al., 2006), polymethylmethacrylate (Gogna et al., 2007), hyaluronic acid benzyl ester (Anselmi et al., 2002), ethylcellulose and PLGA (Perugini et al., 2002) delivery systems greatly enhanced their performance. Chitosan is another polymer widely investigated as a versatile carrier matrix for the delivery of drugs and cosmetic materials (Paolicelli, de la Fuente, Sánchez, Begoña, & Alonso, 2009). Chitosan shows skin compati-

* Corresponding author at: Strathclyde Institute of Pharmacy and Biomedical Sciences, University of Strathclyde, 27 Taylor Street, Glasgow, G4 0NR, Scotland, UK. Tel.: +44 07861431795; fax: +44 01415522562.
E-mail addresses: yasmine87ag@yahoo.com, yasmine.gomaa@strath.co.uk (Y.A. Gomaa), lakhalil@gmail.com (L.K. El-Khordagui), nboraie@yahoo.com (N.A. Boraei), inas_abd.elmonem@yahoo.com (I.A. Darwish).
[1] Tel.: +20 12 3105286; fax: +20 3 4873273.
[2] Tel.: +20 10 1354603; fax: +20 3 4873273.
[3] Tel.: +20 10 5355497; fax: +20 3 4873273.

0144-8617/$ – see front matter © 2010 Elsevier Ltd. All rights reserved.
doi:10.1016/j.carbpol.2010.02.024

bility and adhesive properties (Shimoda, Onishi, & Machida, 2001), water resistance enhanced by crosslinking (Lim & Wan, 1995) as well as UV absorption (Anumansirikul, Wittayasuporn, Klinubol, Tachaprutinum, & Wanichwecharungruang, 2008). Hence, chitosan potentially satisfy the requirements of a good polymer matrix for the delivery of sunscreens especially hydrophilic agents.

Phenylbenzimidazole sulphonic acid (PBSA, Ensulizole, USA) is an authorized hydrophilic relatively photostable UV-B filter (Couteau, Faure, Fortin, Paparis, & Coiffard, 2007) commonly used in cosmetic products at a maximum concentration of 8% (w/w) with no skin irritation or photosensitization potential (COLIPA, 2006). Because of its water solubility, it is added to the water phase in emulsion systems and used in clear gels, resulting in aesthetically pleasing moisturizing sunscreen formulations with light skin feeling. PBSA was reported to boost the photoprotective effect of other organic and inorganic sunscreens (Johncock, 1999). However, PBSA was reported to generate under solar simulated radiation a variety of free radicals and active oxygen species that cause photo-induced damage to DNA in vitro (Inbaraj, Bilski, & Chignell, 2002). The inclusion of PBSA in sunscreen formulations and its overall sunscreen performance, particularly sustained delivery may be enhanced by incorporation in an appropriate delivery system.

The objective of this study was to combine the potentials of PBSA as a hydrophilic molecular UV absorber with those of chitosan as an active matrix material in a simple microparticulate delivery system with desirable characteristics.

2. Materials and methods

2.1. Materials

Phenylbenzimidazole sulphonic acid (NEO HELIOPAN® HYDRO/USP) was kindly provided by Symrise GmbH + Co. KG, Germany. Chitosan (minimal of 85% degree of deacetylation) and sorbitan trioleate (Span 85) were purchased from Sigma–Aldrich Chemie GmbH, Germany. Glutaraldhyde 25% (w/v) was obtained from Fluka Chemie GmbH, Germany. Sodium acetate trihydrate, sodium hydroxide, glacial acetic acid, petroleum ether and liquid paraffin were obtained from El-Nasr Pharmaceutical Co., Egypt. Transpore™ tape was purchased from International Biomedical Group, Egypt.

2.2. Preparation of chitosan microparticles (MPs)

Chitosan MPs were prepared using the emulsion crosslinking method (Kumbar, Kulkarni, & Aminabhavi, 2002). Chitosan solution (4%, w/v in 5%, v/v glacial acetic acid) was added portion wise to 200 ml liquid paraffin containing Span 85 (2%, w/v) with stirring at 4000 rpm (Arrow mechanical stirrer, model 6000, Arrow engineering Co., Pennsylvania). Stirring was continued at the same speed for 5 min after the last addition of the chitosan solution. Glutaraldehyde, 25% (w/v) was added to the mixture with continuous stirring at the same speed for another 3 min. Stirring was continued afterwards for 1 h at a reduced speed (600 rpm). Suspensions of the formed chitosan MPs in liquid paraffin were allowed to settle by standing for 30 min. The clear supernatant was decanted and the MPs obtained as a residue were washed 4 times with petroleum ether. MPs were then allowed to air dry. Each batch was prepared in duplicate. The air dried MPs were collected and stored in a desiccator at ambient temperature (≈25 °C).

Loaded MPs were prepared by dispersion of PBSA in the chitosan solution prior to emulsification. Four test formulations with different PBSA:chitosan ratios and added amount of glutaraldehyde (in terms of volume of 25%, w/v solution) were prepared (Table 1).

2.3. Scanning electron microscopy (SEM)

MPs were mounted onto metal stubs using double-sided adhesive tape onto which the MPs were sprinkled. The stubs were then coated with gold using a sputter coater (JEOL, model JFC-1100E, Japan).

2.4. PBSA microparticles content and percentage incorporation efficiency (% I.E.)

PBSA MPs were suspended in 0.02% (w/v) sodium hydroxide to extract the drug form the microparticles (COLIPA, 2006). After 24 h, the solution was filtered and the filtrate was analyzed spectrophotometrically at 310 nm for the drug content (Shimatzu, model UV-1601 PC, Japan). The % I.E. was calculated as the mean actual sunscreen content divided by the theoretical sunscreen content multiplied by 100.

$$\%\ \text{I.E.} = \frac{\text{Actual sunscreen content}}{\text{Theoretical sunscreen content}} \times 100$$

2.5. Microparticle size analysis

MPs were redispersed in water by sonication for 3 min. PBSA-loaded MPs were analyzed for their size and size distribution using a laser diffraction particle size analyzer (Cilas, model 1064 liquid, France). Results were reported as the mean diameters, $D_{90\%}$, $D_{50\%}$, and $D_{10\%}$ (diameters of percentage of particles under size). The size distribution was also estimated using the SPAN factor. Low values of SPAN indicate a narrow distribution of size and low polydispersity (Park, Jeon, Haam, Park, & Kim, 2004).

$$\text{SPAN} = \frac{D_{90\%} - D_{10\%}}{D_{50\%}}$$

2.6. Infrared spectroscopy (IR)

Samples of PBSA, chitosan, plain MPs and PBSA-loaded MPs were mixed in a mortar with KBr and compressed into discs. The discs were scanned from 500 to 4000 cm^{-1} using FTIR spectrometer (Perkin Elmer spectrum RXIFT-IR system, Perkin instruments, U.S.A.).

2.7. Thermal analysis

A differential scanning calorimeter (DSC, PerkinElmer model DSC 6, PerkinElmer instruments, U.S.A.) was used to determine the crystalline state of the formulation components before and after MPs formation. The analysis was performed using PBSA, chitosan flakes, plain and PBSA-loaded MPs. Samples were hermetically sealed in an aluminum pan and heated at a constant rate of 5 °C per min, over a temperature range of 35–330 °C. Inert atmosphere was maintained by purging nitrogen at a flow rate of 20 ml per min.

2.8. In vitro release study

PBSA release from MPs was investigated using a membraneless method. An accurately weighed amount of MPs equivalent to 20 mg of PBSA as well as a control sample of the same amount of PBSA, were suspended in 40 ml acetate buffer pH 5 in capped Erlenmeyer flasks (Torrado, Torrado, & Cadórniga, 1992). A pH 5 release medium has been used to simulate in-use pH conditions of the skin surface (Denet, Vanbever, & Préat, 2004; Schmid-Wendtner & Korting, 2006; Wissing & Müller, 2002). The flasks were agitated in a thermostatically controlled shaking water bath equilibrated

Table 1
Characteristics of PBSA-loaded chitosan MPs prepared using two drug:polymer ratios and two volumes of glutaraldehyde (G) solution 25%.

Formula	Drug:polymer ratio	ml G solution25%	Drug loading, mg/100 mgMPs	% I.E.	Mean diameter, μm	SPAN
F1	1:1	1.2	21.08	42.2	55.8	2.02
F2	2:1	1.2	49.60	74.4	100.0	1.68
F3	1:1	2.4	14.62	29.2	24.3	3.28
F4	2:1	2.4	45.75	68.5	87.2	1.52

at 35 °C ± 0.2 at 50 strokes per min (GFL thermostatically controlled mechanical shaker, type 1083, Germany). At scheduled time intervals, 1 ml samples were withdrawn and analyzed spectrophotometrically at 310 nm after appropriate dilution with 0.02% (w/v) sodium hydroxide. The volume of withdrawn samples was immediately compensated for by the addition of an equal volume of fresh medium pre-equilibrated at 35 °C. All release studies were run in triplicate and mean values of percentage PBSA released calculated after correction for release medium compensation. The mechanism of PBSA release was determined by fitting release data to zero order, first order and Higuchi equations.

2.9. *In vitro assessment of the UV screening effect of PBSA–chitosan microparticles gel using Transpore™ tape as a substrate*

The method is based on the measurement of UV radiation transmitted through Transpore™ tape as a substrate covered with a film of the sunscreen preparation (Diffey & Robson, 1989). PBSA–chitosan MPs in chitosan gel (4%, w/v in 5%, v/v glacial acetic acid) was applied on the surface of the Transpore™ tape at a 2 mg per cm^2 application thickness. 2% free PBSA in chitosan gel (4%, w/v in 5%, v/v glacial acetic acid), Plain chitosan gel, chitosan gel containing plain chitosan MPs (in a proportion equal to that added in case of loaded MPs) were used for comparison. Transmission was measured from 290 to 400 nm at intervals of 5 nm at five separate locations as well as for a control Transpore™ tape. Spectra with the lowest and the highest transmission were discarded ending up with a set of three spectra. The monochromatic protection factor (MPF) was determined at each wavelength by dividing the transmittance of the control Transpore™ substrate by that of the substrate with applied formulation. The predicted SPF was calculated according to the following formula:

$$\text{In vitro SPF Transpore}^{TM} = \frac{\sum_{290\,nm}^{400\,nm} E(\lambda)\cdot\varepsilon(\lambda)}{\sum_{290\,nm}^{400\,nm} E(\lambda)\cdot\varepsilon(\lambda)/\text{MPF}(\lambda)}$$

where: $E(\lambda)$ is the spectral irradiance of terrestrial sunlight under defined conditions, $\varepsilon(\lambda)$ is the relative effectiveness of UV radiation at wavelength λ nm in producing delayed erythema in human skin (erythemal effectiveness), MPF(λ) is the monochromatic protection factor at wavelength λ nm.

3. Results and discussion

PBSA-loaded chitosan MPs were obtained using an emulsion crosslinking method using glutaraldehyde. This involves a Schiff base reaction between the two aldehydic groups of glutaraldehyde and the amino groups of chitosan forming covalent imine bonds (Jayakrishnan & Jameela, 1996). At the end of the preparation and washing procedures, chitosan MPs were obtained with a yield of 76%.

3.1. *Scanning electron microscopy (SEM)*

SE micrographs of plain chitosan MPs hardened at two glutaraldehyde levels are shown in Fig. 1. Microparticles were spherical with smooth, non-porous and more or less dampled surfaces. Increasing the crosslinking level did not considerably affect MPs surface properties. Incorporation of PBSA into MPs altered their morphology to a great extent (Fig. 2(a)–(d)). At the lower sunscreen payload (1:1 drug:chitosan ratio, F1 and F3, Fig. 2(a) and (b), MPs exhibited a more irregular shape and rougher surface. Increasing the sunscreen payload (2:1 drug:chitosan ratio, F2 and F4, Fig. 2(c) and (d) resulted in increased surface roughness and shape irregularities associated with surface deposition of rod-shaped PBSA crystals (Fig. 2(e) and (f)).

3.2. *PBSA microparticles content and percentage incorporation efficiency (% I.E.)*

The sunscreen content and % I.E. of PBSA-loaded chitosan MPs were affected by both the drug:polymer ratio and the added amount of glutaraldehyde (in terms of volume of 25%, w/v solu-

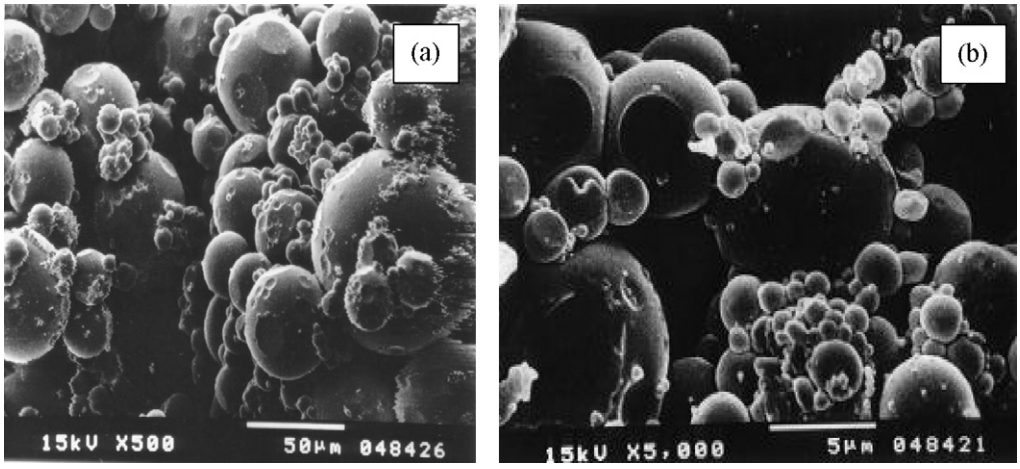

Fig. 1. SEM of plain chitosan microparticles: (a) 1.2 ml and (b) 2.4 ml 25% glutaraldehyde solution.

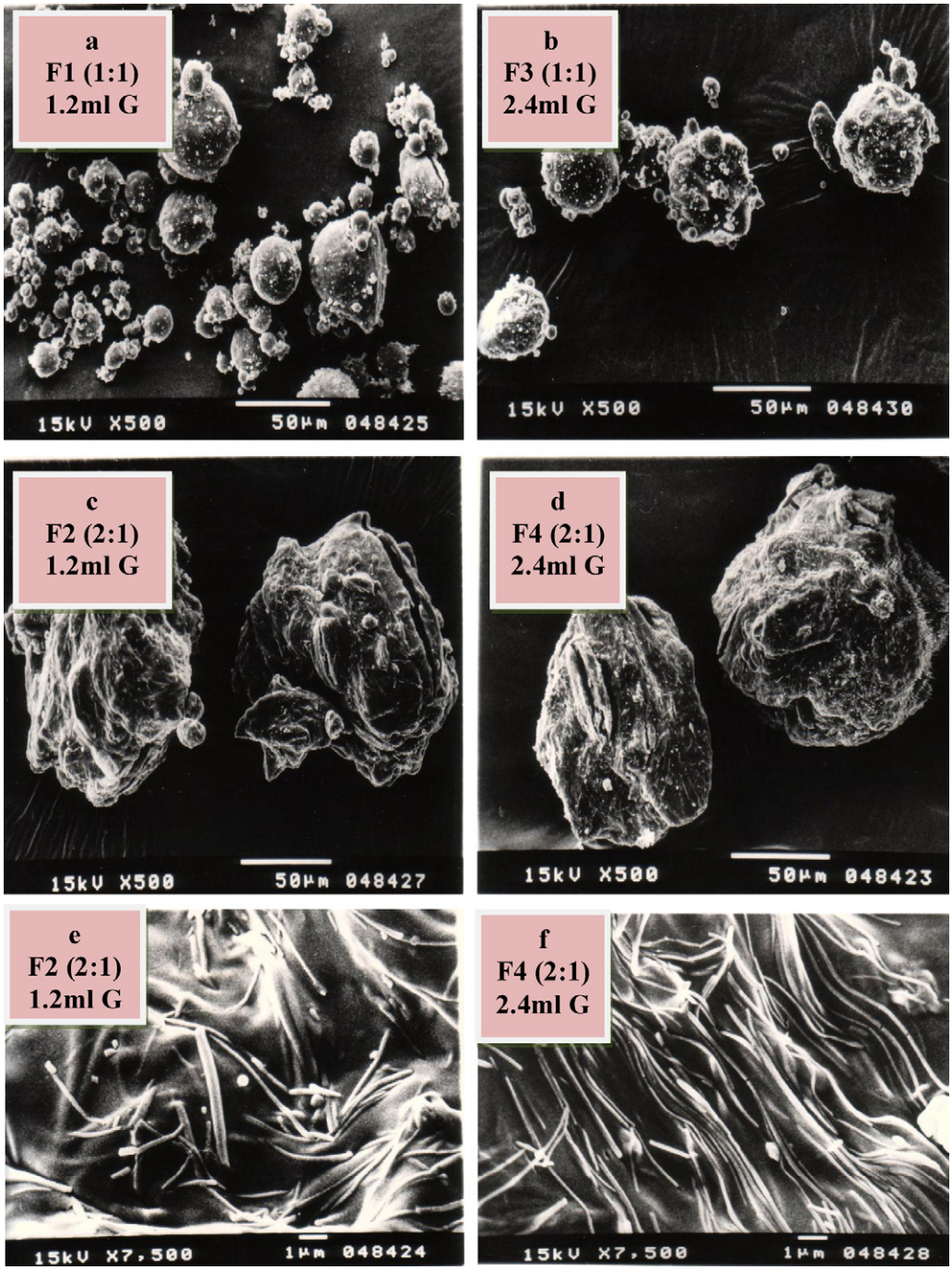

Fig. 2. SEM of PBSA-loaded chitosan MPs.

tion) as shown in Table 1. Doubling the drug:chitosan ratio at a fixed glutaraldehyde level led to increased drug content and % I.E. This was likely because of the insolubility of PBSA in the external emulsion phase (liquid paraffin) and its availability for entrapment within the chitosan matrix. On the other hand, increasing the level of glutaraldehyde resulted in decreased PBSA content which was less pronounced at higher drug:chitosan ratio (F3 and F4, Table 1). This could be attributed to the observed decrease in the MPs size (Table 1) and reduction in the amount of PBSA that could be accommodated. A rank order correlation was observed between microsphere size and their drug loading or % I.E. (Table 1).

3.3. Microparticles size analysis

Data indicated that MPs size was influenced by PBSA:chitosan ratio and the amount of glutaraldehyde used for crosslinking and that polydispersity was generally reduced by increasing the initial PBSA loading. An increase in mean diameter was observed at the higher drug loading which could be attributed to the higher viscosity of the chitosan dispersed phase during MPs preparation which reduces the efficiency of the emulsification process (He, Davis, & Illum, 1999).

Comparison of data for PBSA–chitosan MPs prepared at the same sunscreen loading and different levels of glutaraldehyde (F3 *ver-*

sus F1) and (F4 *versus* F2) indicated a marked reduction in mean diameters particularly at the lower loading (Table 1). Increased chitosan matrix density at higher crosslinker concentrations was shown to be associated with microsphere size reduction (Rokhade, Shelke, Patil, & Aminabhavi, 2007). Although glutaraldehyde would preferentially interact with the free amino groups of chitosan, the less pronounced size reduction at higher drug loading could be attributed to a PBSA–glutaraldehyde interaction that interferes with the crosslinking process. Interaction of glutaraldehyde with other drug molecules containing groups capable of forming Schiff base with aldehydes was reported (He et al., 1999). Glutaraldehyde–PBSA interaction in the present study was investigated by IR spectroscopy.

3.4. Infrared spectroscopy (IR)

Crosslinking of chitosan with glutaraldehyde produced marked changes in the IR spectrum of both chitosan and PBSA as a result of chitosan–PBSA–glutaraldehyde interactions (Fig. 3). The IR spectrum of PBSA showed characteristic strong peaks at 3366 cm^{-1} (N–H stretching), 1632 cm^{-1} (N–H bending), and 2 other bands at 1226 cm^{-1} and 1175 cm^{-1} (C=N stretching). The main chitosan IR spectral characteristics are a broad strong peak at 3435 cm^{-1} (N–H and O–H stretching vibration) in addition to 2 characteristic peaks at 1631 cm^{-1} (N–H bending) and 1384 cm^{-1} (C–O stretching) (Furniss, Hannaford, Smith, & Tatchell, 1989). Crosslinking of chitosan with glutaraldehyde during MPs formation resulted in a reduction in the peak intensity at 3435 cm^{-1}. This is attributed to the formation of Schiff base with the –CHO group of glutaraldehyde, an interaction leading to disappearance of the band component responsible for the N–H stretching of chitosan. Moreover, the crosslinking process caused the N–H bending band in chitosan to split into 2 bands at 1631 cm^{-1} and 1508 cm^{-1}, an observation reported previously (Agnihotri & Aminabhavi, 2004). Incorporation of PBSA in chitosan MPs caused a further reduction in the peak intensity at 3435 cm^{-1} (F1, Fig. 3), which could be ascribed to a chitosan–PBSA interaction involving the O–H stretching band component with possible formation of an ester linkage with the PBSA sulphonic group. This is evidenced by the disappearance of the chitosan O–H stretching band at the higher drug:polymer ratio (F2, Fig. 3).

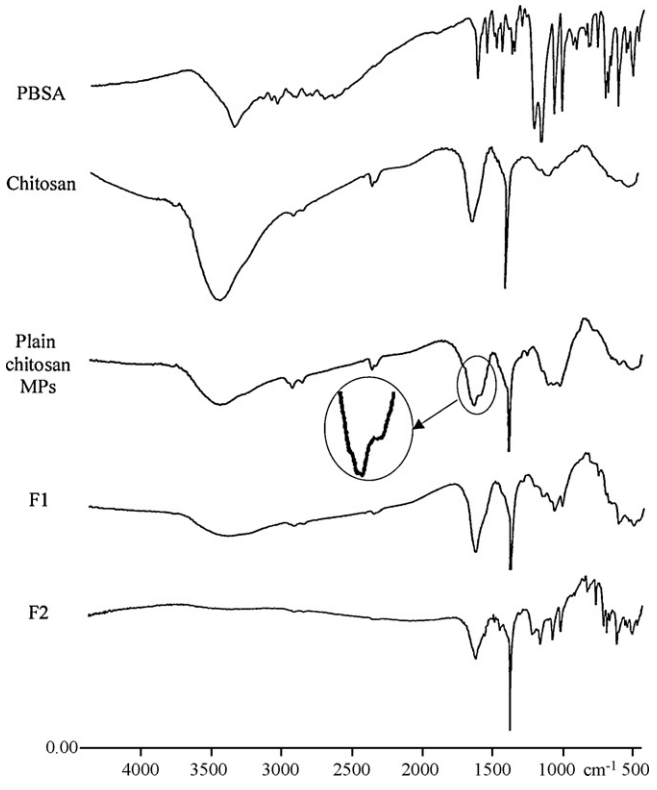

Fig. 3. IR spectra of PBSA, chitosan, plain and loaded MPs.

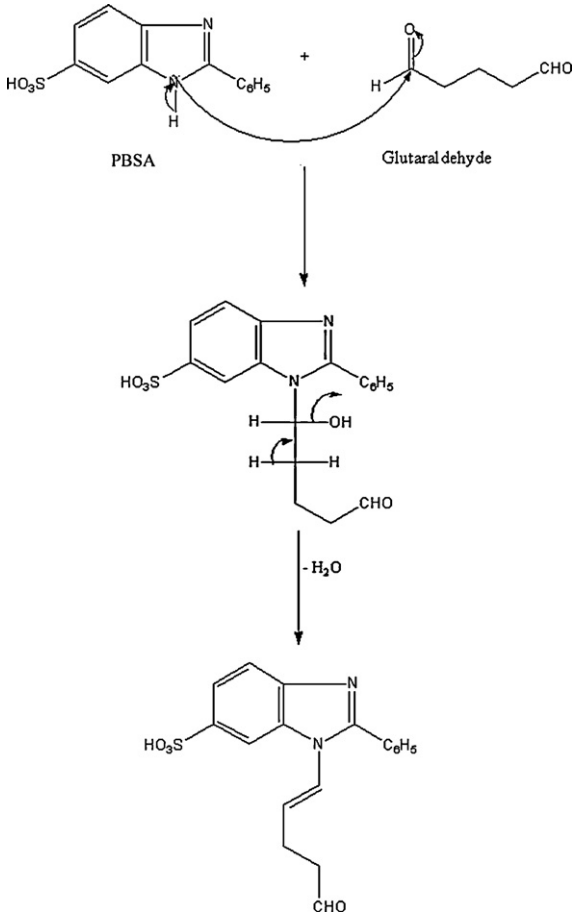

Fig. 4. Electrophillic addition reaction between PBSA and glutaraldhyde.

On the other hand, the finger print spectral characteristics of PBSA incorporated in MPs were masked by those of chitosan (Fig. 3). The disappearance of the N–H stretching band a 3366 cm^{-1}, especially at the higher drug loading (F2, Fig. 4) may be attributed to an electrophilic addition reaction between the aromatic –NH of PBSA and the –CHO of glutaraldehyde, which could explain, at least in part, the particle size analysis data obtained. A possible mechanism is shown in Fig. 4.

3.5. Thermal analysis

DSC thermograms of PBSA-loaded chitosan microspheres (F1 and F2) and their individual components are shown in Fig. 5. PBSA showed an endothermic peak at 98.8 °C while chitosan showed a large endotherm over the temperature range of 74.6–107.9 °C representing the energy required for water vaporization. Such endotherms are typical of amorphous hydrated substances including chitosan which have high affinity for water (Mucha & Pawlak, 2005; Shantha & Harding, 2002). The absence of other endotherms implies that chitosan MPs are amorphous in nature. The exotherm observed at 306.3 °C in the DSC thermogram of chitosan corresponds to chemical decomposition of the polymer (El Gibaly, 2002). Shift of the exotherm to lower temperatures in the DSC profiles of chitosan microspheres (F1 and F2) indicate that process-

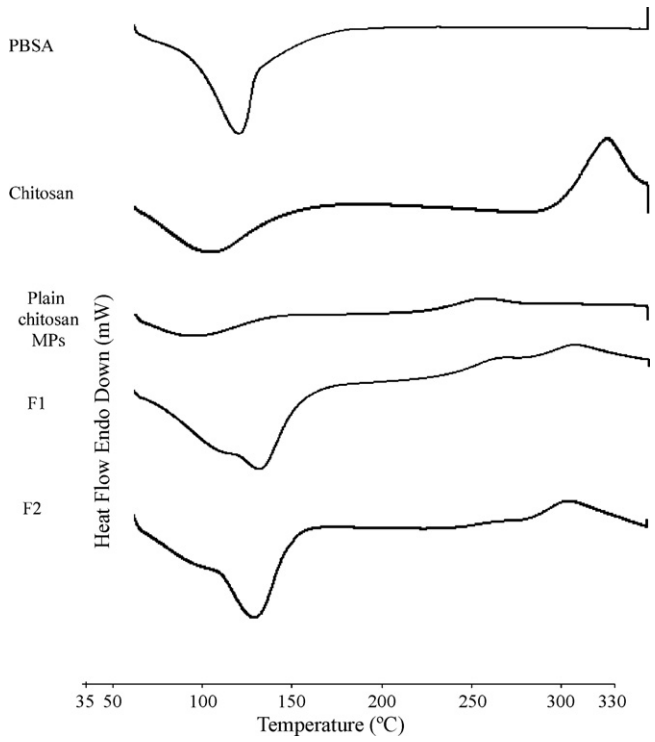

Fig. 5. DSC thermograms of PBSA, chitosan, plain and loaded MPs.

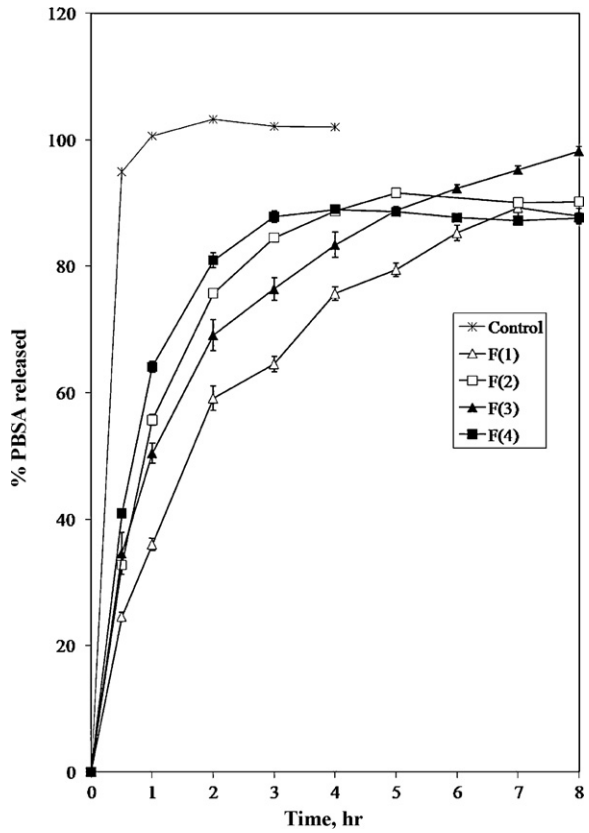

Fig. 6. Release profiles of PBSA-loaded chitosan microparticles in acetate buffer pH 5 at 35 °C.

ing of chitosan into MPs may facilitate its chemical degradation as described previously (Lim & Wan, 1995). It was observed that the endothermic peak of PBSA was preserved in MPs formulas although a slight shift to higher temperature in thermograms of drug-loaded MPs could be observed. Data indicated lack of change of the crystalline state of PBSA upon incorporation in chitosan microparticles.

3.6. *In vitro release study*

Drug release from chitosan MPs would depend on the interplay of the characteristics of the polymer matrix, in terms of degree of crosslinking, porosity, swellability and drug–matrix interactions, the drug solubility in the release medium and the MPs size. Release profiles of free and PBSA-loaded chitosan MPs in pH 5 acetate buffer at 35 °C are shown in Fig. 6. Free PBSA (control) showed 100% dissolution in 1 h. Despite hydrophilicity of both PBSA and the chitosan matrix, entrapment of PBSA in chitosan MPs reduced the rate and cumulative amount of drug released producing biphasic release profiles lacking an extensive immediate burst effect. This suggests that PBSA was mainly densely entrapped near the MPs periphery rather than adsorbed at their surface. Profiles showed a relatively fast initial release extending over at least 2 h, followed by sustained delivery over a period of 8 h. Such profiles are adequate as far as in-use requirements are concerned and point to the potential of the delivery system to allow for a relatively rapid photoprotective effect that could be maintained over a practically reasonable duration. Compared to the release profile of F1 MPs (1:1 drug:chitosan ratio at the lower level of glutaraldehyde), F2 MPs with a higher drug loading (2:1) at the same level of crosslinker showed a faster initial release rate. A larger amount of PBSA near or at the MPs surface as evidenced by SEM (Fig. 2(e)) may account for the observation. Drug release from delivery systems usually increases by increasing drug loading (Sinha et al., 2004). At higher drug loading, the thickness of the matrix material decreases as the amount of polymer decreases, resulting in accelerated penetration of the release medium and solubilization of the entrapped material (Filipovic-Grcic et al., 2003).

Although the increase in the amount of crosslinking agent usually results in reduced release rate of entrapped drugs (Gupta & Jabrail, 2006; Jameela & Jayakrishnan, 1995), a limited increase in the release rate of PBSA was noted in this study, particularly at the lower drug:polymer ratio. A slight difference was noted at the higher drug loading. Increasing the concentration of glutaraldehyde resulted in marked reduction of particle size (Table 1) and the release profile may be considered the resultant of the effects of increasing glutaraldehyde concentration on the inner matrix density leading to release retardation and the reduced MP size leading to release enhancement. Nevertheless, increased drug release at higher extent of crosslinking has been previously reported (Wang, Ma, & Su, 2005).

The mode of PBSA release from chitosan MPs with 1:1 drug:polymer ratio and 2 crosslinking levels (F1 and F3) were studied. Fig. 6 showed lack of fit of the release data to the zero order kinetics. Data were further plotted as log (drug remaining in the matrix) *versus* time and % drug released *versus* square root of time graphs (Fig. 7(a) and (b) respectively). The curves obtained were regressed. The values of "R^2" for F1 plot were 0.984 and 0.986, respectively, and for F3 plot 0.989 and 0.976, respectively. Relatively high and nearly equal correlation coefficients were obtained and a more stringent test was needed to distinguish between dissolution and diffusion mechanisms. Data were plotted as release rate (dQ/dt) of PBSA *versus* Q and $1/Q$ respectively (Fig. 7(c) and (d) respectively), where Q is the amount of PBSA released (Akbuga, 1991). Higher correlation coefficients (0.983 for F1 and 0.985 for F3) were obtained for rate *versus* Q plots indicating that the release of PBSA from chitosan MPs was governed by first order kinetics i.e. dissolution controlled.

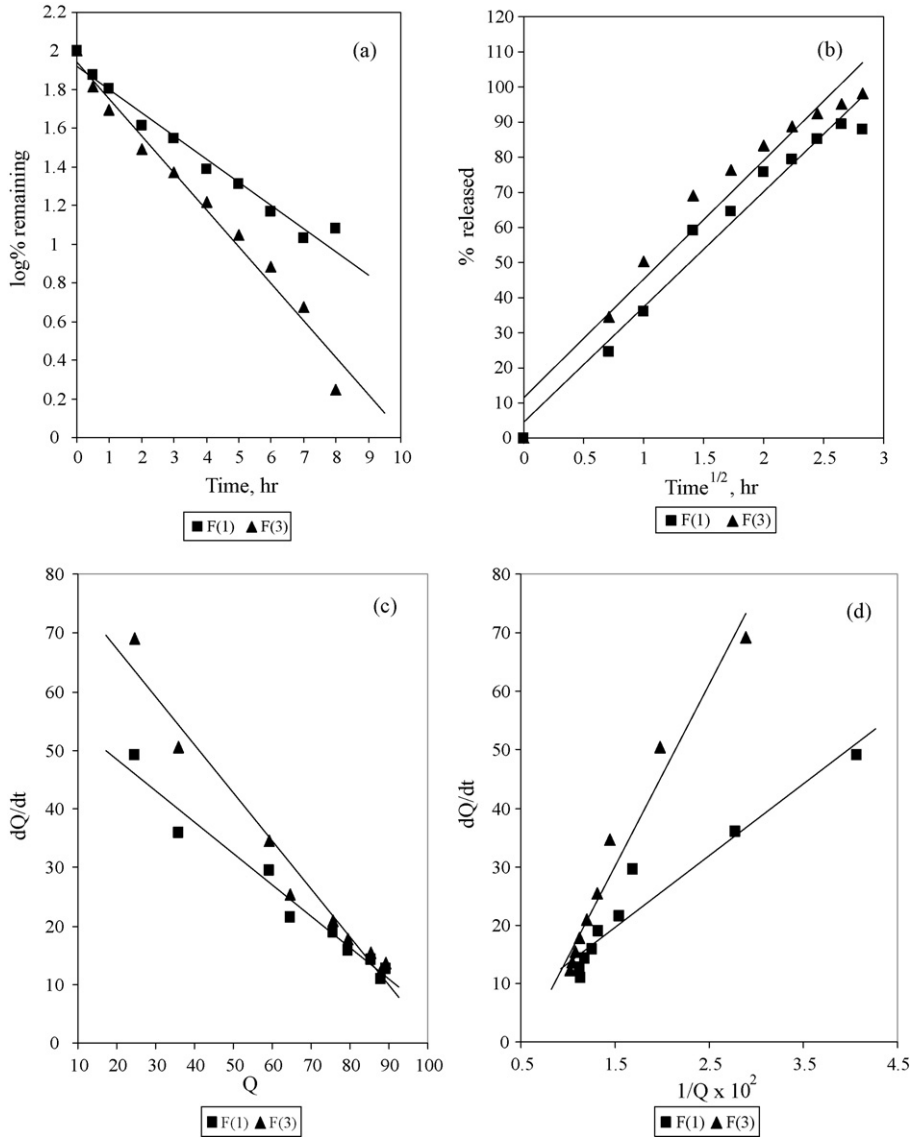

Fig. 7. Release kinetic plots of F1 and F3 MPs.

Attempts to apply first order and Higuchi diffusion model to release data from MPs with a higher drug loading (F2 and F4) resulted in non-linear plots. Initial release points deviated from linearity, probably as a result of release of PBSA located at or near the surface of microspheres. Higuchi square root equation was shown to apply only to matrix systems containing relatively high proportion of the polymer (Hasan, Najib, Suleiman, El-Sayed, & Abdel-Hamid, 1992).

3.7. *In vitro assessment of the ultraviolet effect of PBSA–chitosan microparticles gel using Transpore™ tape as a substrate*

Transpore™ tape was selected as a substrate for in vitro determination of UV screening because of its uneven topography that allows distribution of the sunscreen film in a way similar to human skin, low cost, ready availability, and ease of use (Diffey & Robson, 1989). A MPs formula (F1) with good potentials for product formulation was selected for UV screening assessment. Selection was based on a particle size that precludes skin mechanical irritation and absorption (mean diameter 55.8 μm), an adequately high PBSA incorporation efficiency (42.2%) in addition to a favorable drug release profile. F1 MPs containing 2% PBSA were incorporated in a model 4% chitosan gel as a test formulation. Other test formulations prepared with the same gel base were used for comparison. Data indicated that plain chitosan gel did screen UV radiation in the 290–400 nm range with a calculated in vitro SPF of 0.89 (Fig. 8). Crosslinking of chitosan slightly increased the UV screening effect as indicated by the slightly higher SPF of plain chitosan MPs gel (0.93). Incorporation of 2% free PBSA in the gel increased the SPF from 0.89 to 1.14 while incorporation of the drug at the same concentration level loaded in chitosan MPs further raised the SPF to 1.61 (Fig. 8). The relatively low SPF values obtained for the test PBSA formulations can be attributed to the relatively low intrinsic UV screening effect of PBSA at concentrations lower than 3% (Environmental Working Group, 2009). Despite low values, the calculated SPF could adequately indicate the relative UV screening effect of the test formulations for the purpose of this study. It is worth noting that PBSA is used in higher concentrations in sunscreen products (up to 8%) usually in combination with other organic and inorganic sunscreen actives (Johncock, 1999) to improve the product attributes and achieve high SPF values.

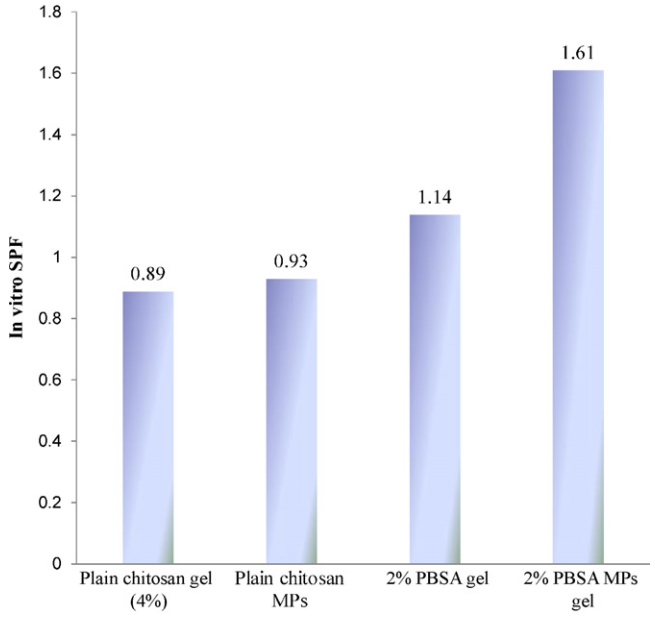

Fig. 8. In vitro Sun Protection Factors (SPF) of tested MPs formulations.

4. Conclusion

Chitosan, a hydrophilic polymer with potentials as a carrier system for hydrophilic sunscreen agents was used to prepare PBSA-loaded chitosan microparticle delivery system using an emulsification crosslinking method. The system characteristics, in terms of size, % I.E. and drug release proved to be influenced by the interplay of the density of crosslinked chitosan matrix as determined by the amount of crosslinker, particle size and chitosan–glutaraldehyde–PBSA interactions as evidenced by FTIR and DSC. The sunscreen release profile at skin pH generally meets in-use requirements. The UV screening effect of a test chitosan gel increased by incorporating PBSA as drug-loaded chitosan microparticles. Accordingly, chitosan microparticles combining the advantages of PBSA as hydrophilic sunscreen and chitosan as active matrix material may contribute to the formulation improvement of sunscreen products.

References

Agnihotri, S. A., & Aminabhavi, T. M. (2004). Controlled release of clozapine through chitosan microparticles prepared by a novel method. *Journal of Control Release*, *96*, 245–259.

Akbuga, J. (1991). Furosemide-loaded ethyl cellulose microspheres prepared by spherical crystallization technique: Morphology and release characteristics. *International Journal of Pharmaceutics*, *76*, 193–198.

Anselmi, C., Centini, M., Rossi, C., Ricci, M., Rastrelli, A., Andreassi, M., et al. (2002). New microencapsulated sunscreens: Technology and comparative evaluation. *International Journal of Pharmaceutics*, *242*, 207–211.

Anumansirikul, N., Wittayasuporn, M., Klinubol, P., Tachaprutinun, A., & Wanichwecharungruang, S. (2008). UV-screening chitosan nanocontainers: Increasing the photostability of encapsulated materials and controlled release. *Nanotechnology*, *19*, 1–9.

Chunjin, S., & Shuangxi, L. (2005). A new healthy sunscreen system for human: Solid lipid nanoparticles as carrier for 3,4,5-trimethoxy-benzoylchitin and the improvement by adding Vitamin E. *International Journal of Biological Macromolecules*, *36*, 116–119.

COLIPA. (2006). *Opinion on phenylbenzimidazole sulfonic acid and its salts*. Opinion adopted by the SCCP, S45.

Couteau, C., Faure, A., Fortin, J., Paparis, E., & Coiffard, L. (2007). Study of the photostability of 18 sunscreens in creams by measuring the SPF in vitro. *Journal of Pharmaceutical and Biomedical Analysis*, *44*, 270–273.

Denet, A. R., Vanbever, R., & Préat, V. (2004). Skin electroporation for transdermal and topical delivery. *Advanced Drug Delivery Reviews*, *56*, 659–674.

Diffey, B. L., & Robson, J. (1989). A new substrate to measure sunscreen protection factors throughout the ultraviolet spectrum. *Journal of the Society of Cosmetic Chemists*, *40*, 127–133.

El Gibaly, I. (2002). Development and in vitro evaluation of novel floating chitosan microcapsules for oral use: Comparison with non-floating chitosan microspheres. *International Journal of Pharmaceutics*, *249*, 7–21.

Environmental Working Group. (2009). Ensulizole (Phenylbenzimidazole sulphonic acid) available at: http://www.cosmeticsdatabase.com/ingredient.php?ingred06=702252. Accessed on August 2009.

Filipovic-Grcic, J., Perissutti, B., Moneghini, M., Voinovich, D., Martinac, A., & Jalsenjak, I. (2003). Spray-dried carbamazepine-loaded chitosan and HPMC microspheres: Preparation and characterisation. *Journal of Pharmacy and Pharmacology*, *55*, 921–931.

Forestier, S. (2008). Rationale for sunscreen development. *Journal of the American Academy of Dermatology*, *58*, 134S–138S.

Fourtanier, A., Moyal, D., & Seité, S. (2008). Sunscreen containing the broad spectrum UVA absorber, Meroxyl SX, prevent the cutaneous detrimental effects of UV exposure: A review of clinical study results. *Photodermatology Photoimmunolology & Photomedicine*, *24*, 164–174.

Furniss, B. S., Hannaford, A. J., Smith, P. W. G., & Tatchell, A. R. (1989). Specroscopic methods and the interpretation of spectra. In *Vogel's textbook of practical organic chemistry*. England: Longman Group UK Ltd., pp. 254–316

Gogna, D., Jain, S., Yadav, A., & Agrawal, G. (2007). Microsphere based improved sunscreen formulation of ethylhexyl methoxycinnamate. *Current Drug Delivery*, *14*, 153–159.

González, S., Fernández-Lorente, M., & Gilaberte-Calzada, Y. (2008). The latest on skin photoprotection. *Clinics in Dermatology*, *26*, 614–626.

Gupta, K. C., & Jabrail, F. H. (2006). Effects of degree of deacetylation and cross-linking on physical characteristics, swelling and release behavior of chitosan microspheres. *Carbohydrate Polymers*, *66*, 43–54.

Hasan, M., Najib, N., Suleiman, M., El-Sayed, Y., & Abdel-Hamid, M. (1992). In vitro and in vivo evaluation of sustained-release and enteric-coated microcapsules of diclofenac sodium. *Drug Development and Industrial Pharmacy*, *18*, 1981–1988.

He, P., Davis, S. S., & Illum, L. (1999). Chitosan microspheres prepared by spray drying. *International Journal of Pharmaceutics*, *187*, 53–65.

Iannuccelli, V., Sala, N., Tursilli, R., Coppi, G., & Scalia, S. (2006). Influence of lipospheres preparation on butyl-methoxydibenzoylmethane photostability. *European Journal of Pharmaceutics and Biopharmaceutics*, *63*, 140–145.

Inbaraj, J., Bilski, P., & Chignell, C. (2002). Photophysical and photochemical studies of 2-phenylbenzimidazole and UVB sunscreen 2-phenylbenzimidazole sulfonic acid. *Photochemistry and Photobiology*, *75*, 107–116.

Jameela, S. R., & Jayakrishnan, A. (1995). Glutaraldehyde cross-linked chitosan microspheres as a long acting biodegradable drug delivery vehicle: Studies on the *in vitro* release of mitoxantrone and *in vivo* degradation of microspheres in rat muscle. *Biomaterials*, *16*, 769–775.

Jayakrishnan, A., & Jameela, S. R. (1996). Glutaraldhyde as a fixative in bioprostheses and drug delivery matrices. *Biomaterials*, *17*, 471–484.

Johncock, W. (1999). Sunscreen interactions in formulations. *Cosmetics & Toiletries*, *114*, 75–82.

Kumbar, S. G., Kulkarni, A. R., & Aminabhavi, T. M. (2002). Crosslinked chitosan microspheres for encapsulation of diclofenac sodium: Effect of crosslinking agent. *Journal of Microencapsulation*, *19*, 173–180.

Lautenschlager, S., Wulf, H., & Pittelkow, M. (2007). *Photoprotection: The Lancet*, *370*, 528–537.

Lim, L. Y., & Wan, L. S. (1995). Heat treatment of chitosan films. *Drug Development and Industrial Pharmacy*, *21*, 839–846.

Mucha, M., & Pawlak, A. (2005). Thermal analysis of chitosan and its blends. *Thermochimica Acta*, *427*, 69–76.

Nohynek, G., Lademann, J., Ribaud, C., & Roberts, M. (2007). Grey Goo on the Skin? Nanotechnology. Cosmetic and Sunscreen Safety. *Critical Reviews in Toxicology*, *37*, 251–277.

Paolicelli, P., de la Fuente, M., Sánchez, A., Begoña, S., & Alonso, M. (2009). Chitosan nanoparticles for drug delivery to the eye. *Expert Opinion on Drug Delivery*, *6*, 239–253.

Park, S. B., Jeon, Y. J., Haam, S., Park, H. Y., & Kim, W. S. (2004). Preparation of chitosan microspheres using membrane emulsification and its size modelling. *Journal of Microencapsulation*, *21*, 539–552.

Patel, M., Jain, S., Yadav, A., Gogna, D., & Agrawal, G. (2006). Preparation and characterization of oxybenzone-loaded gelatin microspheres for enhancement of sunscreening efficacy. *Drug Delivery*, *13*, 323–330.

Perugini, P., Simeoni, S., Scalia, S., Genta, I., Modena, I., Conti, B., et al. (2002). Effect of nanoparticles encapsulation on the photostability of the sunscreen agent, 2-ethylhexyl-p-methoxycinnamate. *International Journal of Pharmaceutics*, *246*, 37–45.

Rokhade, A., Shelke, N., Patil, S., & Aminabhavi, T. (2007). Novel interpenetrating polymer network microspheres of chitosan and methylcellulose for controlled release of theophylline. *Carbohydrate Polymers*, *69*, 678–687.

Scalia, S., & Mezzena, M. (2009). Co-loading of a photosensitizer with the sunscreen agent, butyl methoxydibenzoylmethane in solid lipid microparticles. *Drug Development and Industrial Pharmacy*, *35*, 192–198.

Schmid-Wendtner, M. H., & Korting, H. C. (2006). The pH of the skin surface and its impact on the barrier function. *Skin Pharmacology and Physiology*, *19*, 296–302.

Shantha, K. L., & Harding, D. R. K. (2002). Synthesis and characterization of chemically modified chitosan microspheres. *Carbohydrate Polymers*, *48*, 247–253.

Shimoda, J., Onishi, H., & Machida, Y. (2001). Bioadhesive characteristics of chitosan microspheres to the mucosa of rat small intestine. *Drug Development and Industrial Pharmacy*, *27*, 567–576.

Sinha, V., Singla, A., Wadhawan, S., Kaushik, R., Kumria, R., Bansal, K., et al. (2004). Chitosan microspheres as a potential carrier for drugs. *International Journal of Pharmaceutics*, *274*, 1–33.

Tanner, P. (2006). Sunscreen product formulation. *Dermatologic Clinics*, *24*, 53–62.

Torrado, S., Torrado, J., & Cadórniga, R. (1992). Topical application of albumin microspheres containing vitamin A: Drug release and availability. *International Journal of Pharmaceutics*, *86*, 147–152.

Touitou, E., & Godin, B. (2008). Skin nonpenetrating sunscreens for cosmetic and pharmaceutical formulations. *Clinics in Dermatology*, *26*, 375–379.

Tuchinda, C., Lim, H., Osterwalder, U., & Rougier, A. (2006). Novel emerging sunscreen technologies. *Dermatologic Clinics*, *24*, 105–117.

Tursilli, R., Piel, G., Delattre, L., & Scalia, S. (2007). Solid lipid microparticles containing the sunscreen agent, octyl-dimethylaminobenzoate: Effect of the vehicle. *European Journal of Pharmaceutics and Biopharmaceutics*, *66*, 483–487.

Velasco, M., Sarruf, F., Salgado-Santos, I., Haroutiounian-Filho, C., Kaneko, T., & Baby, A. (2008). Broad spectrum bioactive sunscreens. *International Journal of Pharmaceutics*, *363*, 50–57.

Villalobos-Hernndez, J., & Muller-Goymann, C. (2007). In vitro erythemal UV-A protection factors of inorganic sunscreens distributed in aqueous media using carnauba wax-decyl oleate nanoparticles. *European Journal of Pharmaceutics and Biopharmaceutics*, *65*, 122–125.

Wang, L., Ma, G., & Su, Z. (2005). Preparation of uniform sized chitosan microspheres by membrane emulsification technique and application as a carrier of protein drug. *Journal of Control Release*, *106*, 62–75.

Wissing, S., & Müller, R. (2002). Solid lipid nanoparticles as carrier for sunscreens: In vitro release and in vivo skin penetration. *Journal of Control Release*, *81*, 225–233.

Xia, Q., Saupe, A., Müller, R. H., & Souto, E. B. (2008). Nanostructured lipid carriers as novel carrier for sunscreen formulations. *International Journal of Cosmetic Science*, *29*, 473–482.